




# Nuclear Hyperfine Mixing Effect in Highly Charged $^{205}\text{Pb}$ Ions

Wu Wang <sup>1</sup>, Yong Li <sup>1,\*</sup> and Xu Wang <sup>2,3,\*</sup>

<sup>1</sup> Center for Theoretical Physics & School of Physics and Optoelectronic Engineering, Hainan University, Haikou 570228, China; wangwu531@hainanu.edu.cn

<sup>2</sup> Graduate School, China Academy of Engineering Physics, Beijing 100193, China

<sup>3</sup> Southern Center for Nuclear-Science Theory, Institute of Modern Physics, Chinese Academy of Sciences, Huizhou 516000, China

\* Correspondence: yongli@hainanu.edu.cn (Y.L.); xwang@giscaep.ac.cn (X.W.)

**Abstract:** In highly charged ions, significant nuclear hyperfine mixing (NHM) effects can arise when the electromagnetic field generated by the electrons interacts strongly with the nucleus, leading to mixing of nuclear states. While previous studies have primarily attributed the NHM effect to unpaired valence electrons, we present a reformulation of the theoretical framework using dressed hyperfine states and investigate the NHM effect in  $^{205}\text{Pb}^{76+}$ ,  $^{205}\text{Pb}^{75+}$ ,  $^{205}\text{Pb}^{74+}$ , and  $^{205}\text{Pb}^{73+}$  ions. Our numerical results show that significant NHM effects occurred in all of the studied ions, even in the absence of unpaired valence electrons in  $^{205}\text{Pb}^{76+}$  and  $^{205}\text{Pb}^{74+}$ . We found that the lifetime of the isomeric state was reduced by 2–4 orders of magnitude compared with the bare  $^{205}\text{Pb}$  nucleus, depending on the charge state of the ion. These results indicate that it is the active valence electrons rather than unpaired electrons which play a key role in the NHM effect, thereby deepening our understanding of this phenomenon.

**Keywords:** nuclear hyperfine mixing; highly charged ions; atomic structure and spectroscopy



Academic Editors: Jean-Christophe Pain, John Sheil and Ronnie Hoekstra

Received: 5 December 2024

Revised: 26 December 2024

Accepted: 2 January 2025

Published: 3 January 2025

**Citation:** Wang, W.; Li, Y.; Wang, X. Nuclear Hyperfine Mixing Effect in Highly Charged  $^{205}\text{Pb}$  Ions. *Atoms* **2025**, *13*, 2. <https://doi.org/10.3390/atoms13010002>

**Copyright:** © 2025 by the authors. Licensee MDPI, Basel, Switzerland. This article is an open access article distributed under the terms and conditions of the Creative Commons Attribution (CC BY) license (<https://creativecommons.org/licenses/by/4.0/>).

## 1. Introduction

Highly charged ions play a fundamental role in the development of atomic structure theory [1], tests on quantum electrodynamics [2–4], and astrophysical diagnostics [5], among other applications. In these ions, pronounced nuclear hyperfine mixing (NHM) effects can occur [6]. Initially referred to as nuclear spin mixing in hyperfine fields, this phenomenon arises when the electrons generate a strong electromagnetic field near the nucleus, leading to mixing of nuclear states [6–8]. A similar phenomenon can also occur in muonic atoms, and it is known as a dynamic hyperfine structure, which has been experimentally observed (see, for example, [9–11] and the references therein). In contrast, the NHM effect in ordinary atoms has not yet been measured. The NHM effect can significantly alter the radiative lifetime of nuclear isomeric states, providing a unique means of actively controlling the nuclear properties [12–18].

The  $^{229}\text{Th}$  nucleus is particularly notable due to its exceptionally low-lying isomeric state of energy near 8.4 eV [19–21]. This makes the NHM effect especially significant [8], particularly in the hydrogen-like ion ( $^{229}\text{Th}^{89+}$ ), where the lifetime of the isomeric state is reduced by five orders of magnitude compared with the bare nucleus [12,14,15]. Typical isomeric energies, however, range from 1 keV to 1 MeV, and it has generally been conjectured that the NHM effect is negligible in nuclei other than  $^{229}\text{Th}$  [7,8]. As a result, research on the NHM effect has been largely limited to highly charged  $^{229}\text{Th}$  ions over the past three decades [8,12–16]. Recent developments in the general theory of NHM have nevertheless revealed that this effect is also significant in  $^{205}\text{Pb}$  [17], which has a 2.329-keV

isomeric state [22]. For the boron-like ion ( $^{205}\text{Pb}^{77+}$ ), the lifetime of the isomeric state is reduced by four orders of magnitude [17]. Moreover, it is commonly believed that unpaired valence electrons play a crucial role in the NHM effect [8]. Consequently, research on the NHM effect has predominantly focused on hydrogen-like, lithium-like, and boron-like ions [8,12–18].

In this work, we investigate the NHM effect in  $^{205}\text{Pb}^{76+}$ ,  $^{205}\text{Pb}^{75+}$ ,  $^{205}\text{Pb}^{74+}$ , and  $^{205}\text{Pb}^{73+}$  ions. We reformulate the theoretical framework of the NHM effect by employing dressed hyperfine states [23], which provide clarity to the discussion. Using the GRASP2018 package [24], we calculate the partial low-lying electronic energy levels of these ions. Although the  $^{205}\text{Pb}^{76+}$  and  $^{205}\text{Pb}^{74+}$  ions lack unpaired valence electrons, our numerical results reveal that significant NHM effects are still present. Compared with the bare nucleus, the lifetime of the isomeric state is reduced by more than two orders of magnitude in  $^{205}\text{Pb}^{76+}$ , by over four orders of magnitude in  $^{205}\text{Pb}^{75+}$ , and by over three orders of magnitude in  $^{205}\text{Pb}^{74+}$  and  $^{205}\text{Pb}^{73+}$ .

## 2. General Theory of NHM

### 2.1. Dressed Hyperfine State

For the combined system of the electrons and the nucleus, the Hamiltonian is given by

$$H = H_e + H_n + H_{\text{en}}, \tag{1}$$

where  $H_e$  and  $H_n$  represent the Hamiltonian of the electrons and the nucleus, respectively.  $H_{\text{en}}$  is the hyperfine interaction, which can be expressed by [25]

$$H_{\text{en}} = \sum_{\tau K} \mathcal{M}^{(\tau K)} \cdot T^{(\tau K)}, \tag{2}$$

where  $\mathcal{M}^{(\tau K)}$  denotes the spherical tensor operator of rank  $K$  ( $K \geq 1$ ) for the nucleus, with its explicit expression provided in [25], and  $T^{(\tau K)}$  represents the spherical tensor operators of rank  $K$  for the electrons. Here,  $\tau = E$  or  $M$  specifies whether these tensor operators are of the electric or magnetic type. The explicit form of  $T^{(\tau K)}$  is given as follows:

$$\begin{aligned} T^{(EK)} &= \int \frac{\rho_e(\mathbf{r})}{r^{K+1}} C^{(K)}(\theta, \phi) d\tau, \\ T^{(MK)} &= \frac{i}{cK} \int \frac{\mathbf{j}_e(\mathbf{r}) \cdot \mathbf{L}[C^{(K)}(\theta, \phi)]}{r^{K+1}} d\tau, \end{aligned} \tag{3}$$

where  $\rho_e(\mathbf{r})$  and  $\mathbf{j}_e(\mathbf{r})$  are the electronic charge density and current density operators, respectively.  $\mathbf{L} = -i\mathbf{r} \times \nabla$  is the orbital angular momentum operator, and  $C^{(K)}$  is a spherical tensor whose components are defined by the spherical harmonics  $Y_{Kq}$  as follows:

$$C_q^{(K)} = \sqrt{\frac{4\pi}{2K+1}} Y_{Kq}, \quad q = -K, -K+1, \dots, K-1, K. \tag{4}$$

In the absence of the hyperfine interaction, the electron-nucleus system can be described by a product state  $|IM_I\rangle|\gamma JM_J\rangle$ , where  $|IM_I\rangle$  represents the nuclear state with nuclear spin  $I$  and  $|\gamma JM_J\rangle$  is the electronic state with electronic angular momentum  $J$ . Here,  $M_I$  and  $M_J$  are magnetic quantum numbers of the nuclear and electronic states, respectively, while  $\gamma$  encompasses all other electronic quantum numbers. When the hyperfine interaction is included,  $I$  and  $J$  are no longer good quantum numbers. Yet, the total angular momentum  $F$ , formed by coupling  $I$  and  $J$ , remains a good quantum number. Consequently, the electron-nucleus system is no longer described by the product state but by the dressed hyperfine state, which is an entangled state between the electrons and the

nucleus. The dressed hyperfine state has been used to describe the hyperfine electronic bridge process and serves as a key tool in the development of the quantum-optical model involving this process [23].

The dressed hyperfine state can be expanded by employing the hyperfine coupled basis [26]

$$|I\gamma J; FM_F\rangle = \sum_{M_I M_J} \langle IM_I J M_J | FM_F \rangle |IM_I\rangle |\gamma J M_J\rangle, \tag{5}$$

where  $M_F$  is the total magnetic quantum number and  $\langle IM_I J M_J | FM_F \rangle$  is the Clebsch–Gordan coefficient. We denote the dressed hyperfine state with a leading term  $|I\gamma J; FM_F\rangle$  as  $|[I\gamma J]FM_F\rangle$ . Based on perturbation theory, this state can be written as follows:

$$|[I\gamma J]FM_F\rangle = |I\gamma J; FM_F\rangle + \sum_{t=1}^{n_h} b_t |I_t \gamma_t J_t; FM_F\rangle, \tag{6}$$

where  $n_h$  denotes the number of the hyperfine coupled basis  $|I_t \gamma_t J_t; FM_F\rangle$  and  $b_t$  is the mixing coefficient between the states  $|I\gamma J; FM_F\rangle$  and  $|I_t \gamma_t J_t; FM_F\rangle$ . Here,  $|I_t \gamma_t J_t; FM_F\rangle$  is a hyperfine coupled basis which differs from  $|I\gamma J; FM_F\rangle$ . In the above equation, the summation over different nuclear states gives rise to the NHM effect. Using Equation (2),  $b_t$  is calculated to be

$$b_t = \sum_{\tau K} \frac{(-1)^{I+J_t+F}}{E - E_t} \begin{Bmatrix} I_t & J_t & F \\ J & I & K \end{Bmatrix} \langle I_t || \mathcal{M}^{(\tau K)} || I \rangle \langle \gamma_t J_t || T^{(\tau K)} || \gamma J \rangle, \tag{7}$$

where  $E$  and  $E_t$  represent the energies of the hyperfine coupled bases  $|I\gamma J; FM_F\rangle$  and  $|I_t \gamma_t J_t; FM_F\rangle$ , respectively. The summation involving  $I_t$  in Equation (6) can be restricted to the nuclear ground state  $I_g$  and the isomeric state  $I_e$  if there are large energy gaps between these states and higher-lying nuclear states. For instance, in the case of  $^{205}\text{Pb}$ , the energy of the isomeric state (first excited state) is 2.329 keV, while the energy of the second excited state lies at 262.8 keV [22].

### 2.2. Nuclear Transition via NHM

Consider a process in which the combined electronic and nuclear system interacts with a radiation field. Initially, the system is in the isomeric state  $|[I_e \gamma_g J_g] F_e M_{F_e}\rangle$ . Through the emission of a photon with energy equal to the nuclear excitation energy  $\omega$ , the system transitions to the nuclear ground state  $|[I_g \gamma_g J_g] F_g M_{F_g}\rangle$ . Here,  $F_g$  ( $F_e$ ) represents the total angular momentum of the nuclear ground (isomeric) state, while  $J_g$  and  $\gamma_g$  denote the angular momentum and all other quantum numbers of the electronic ground state, respectively.

By applying multipole expansion of the radiation field (see, for example, [27]), the nuclear transition rate of type order  $\tau L$  ( $L \geq 1$  is an integer) for the above process is calculated as follows:

$$\Gamma = \frac{2(2L+1)}{[(2L+1)!!]^2} \left(\frac{\omega}{c}\right)^{2L+1} \frac{L+1}{L} \sum_q |\langle [I_g \gamma_g J_g] F_g M_{F_g} | \mathcal{O}_q^{(\tau L)} + \mathcal{M}_q^{(\tau L)} | [I_e \gamma_g J_g] F_e M_{F_e} \rangle|^2, \tag{8}$$

where  $c$  denotes the light speed,  $\mathcal{M}_q^{(\tau L)}$  is the component of the nuclear transition operator  $\mathcal{M}^{(\tau L)}$ , and  $\mathcal{O}^{(\tau L)}$  is the multipole transition operator of the electron:

$$\begin{aligned} \mathcal{O}^{(EL)} &= \frac{1}{\omega(L+1)} \int \mathbf{j}_e(\mathbf{r}) \cdot \nabla \times \mathbf{L} [r^L C^{(L)}(\theta, \phi)] d\tau, \\ \mathcal{O}^{(ML)} &= \frac{-i}{c(L+1)} \int \mathbf{j}_e(\mathbf{r}) \cdot \mathbf{L} C^{(L)}(\theta, \phi) r^L d\tau. \end{aligned} \tag{9}$$

Here,  $C^{(L)}(\theta, \phi)$  is a spherical tensor as given in Equation (4).

By substituting the expansions of states  $||[I_e\gamma_g J_g]F_e M_{F_e}\rangle$  and  $||[I_g\gamma_g J_g]F_g M_{F_g}\rangle$  [given by Equation (6)] into Equation (8), averaging over the initial state, summing over the final state, and using the Wigner–Eckart theorem, the nuclear transition rate  $\Gamma$  can be simplified to

$$\Gamma = 2 \frac{(2L+1)(2F_g+1)}{[(2L+1)!!!]^2} \left(\frac{\omega}{c}\right)^{2L+1} \frac{L+1}{L} |\langle [I_g\gamma_g J_g]F_g || \mathcal{O}^{(\tau L)} + \mathcal{M}^{(\tau L)} || [I_e\gamma_g J_g]F_e \rangle|^2, \quad (10)$$

where the nuclear reduced matrix element  $\langle [I_g\gamma_g J_g]F_g || \mathcal{M}^{(\tau L)} || [I_e\gamma_g J_g]F_e \rangle$  and the electronic reduced matrix element  $\langle [I_g\gamma_g J_g]F_g || \mathcal{O}^{(\tau L)} || [I_e\gamma_g J_g]F_e \rangle$  are given by

$$\begin{aligned} \langle [I_g\gamma_g J_g]F_g || \mathcal{M}^{(\tau L)} || [I_e\gamma_g J_g]F_e \rangle &= \begin{Bmatrix} I_g & I_e & L \\ F_e & F_g & J_g \end{Bmatrix} \langle I_g || \mathcal{M}^{(\tau L)} || I_e \rangle, \\ \langle [I_g\gamma_g J_g]F_g || \mathcal{O}^{(\tau L)} || [I_e\gamma_g J_g]F_e \rangle &= \sum_t \left[ b_{e,t} \begin{Bmatrix} J_g & J_t & L \\ F_e & F_g & I_g \end{Bmatrix} \langle \gamma_g J_g || \mathcal{O}^{(\tau L)} || \gamma_t J_t \rangle \right. \\ &\quad \left. + b_{g,t}^* \begin{Bmatrix} J_t & J_g & L \\ F_e & F_g & I_e \end{Bmatrix} \langle \gamma_t J_t || \mathcal{O}^{(\tau L)} || \gamma_g J_g \rangle \right. \\ &\quad \left. \times (-1)^{J_t - J_g + I_e - I_g} \right]. \end{aligned} \quad (11)$$

Here,  $b_{e,t}$  and  $b_{g,t}$  are the mixing coefficients in the dressed hyperfine states  $||[I_e\gamma_g J_g]F_e M_{F_e}\rangle$  and  $||[I_g\gamma_g J_g]F_g M_{F_g}\rangle$ , respectively. The matrix element  $\langle [I_g\gamma_g J_g]F_g || \mathcal{M}^{(\tau L)} || [I_e\gamma_g J_g]F_e \rangle$  corresponds to direct nuclear transition, which is independent of the electronic transitions. The matrix element  $\langle [I_g\gamma_g J_g]F_g || \mathcal{O}^{(\tau L)} || [I_e\gamma_g J_g]F_e \rangle$  describes the nuclear transition induced by the NHM effect, which depends on the electronic transitions. It should be emphasized that Equation (10) is a general expression including different types of nuclear transitions and mixing coefficients. In contrast, previous works only considered the mixing coefficients corresponding to the electronic ground state [7,8,12–15].

The  $^{205}\text{Pb}$  nucleus has an isomeric state with an energy of 2.329 keV. The spin parity values of the ground and isomeric states are  $5/2^-$  and  $1/2^-$ , respectively. According to angular momentum selection rules, the decay of the isomer in the bare nucleus is dominated by the electric quadrupole (E2) transition, while the magnetic dipole (M1) transition is forbidden. The radiative half-life  $T_{1/2}$  of the isomer in the bare nucleus is approximately 15 min, whereas the nonradiative half-life due to internal conversion is roughly 24.2  $\mu\text{s}$  [22]. For the highly charged  $^{205}\text{Pb}$  ions under consideration, the internal conversion channel is energetically closed, leaving only the radiative decay channel open. The nuclear reduced matrix element  $\langle I_g || \mathcal{M}^{(\tau L)} || I_e \rangle$  is related to the reduced nuclear transition probability by

$$B(\tau L, e \rightarrow g) = \frac{2L+1}{4\pi(2I_e+1)} |\langle I_g || \mathcal{M}^{(\tau L)} || I_e \rangle|^2. \quad (12)$$

In the following calculations, the value of  $B(E2, e \rightarrow g)$  is taken to be 0.127 W.u. [22].

### 3. Results and Discussions

#### 3.1. Energy Levels and Hyperfine Structure of $^{205}\text{Pb}^{76+}$ , $^{205}\text{Pb}^{75+}$ , $^{205}\text{Pb}^{74+}$ , and $^{205}\text{Pb}^{73+}$ Ions

The electronic ground state configurations of the  $^{205}\text{Pb}^{76+}$ ,  $^{205}\text{Pb}^{75+}$ ,  $^{205}\text{Pb}^{74+}$ , and  $^{205}\text{Pb}^{73+}$  ions are  $1s^2 2s^2 2p^2 \ ^3P_0$ ,  $1s^2 2s^2 2p^3 \ ^2P_{3/2}$ ,  $1s^2 2s^2 2p^4 \ ^3P_2$ , and  $1s^2 2s^2 2p^5 \ ^2P_{3/2}$ , respectively. The partial low-lying energy levels of these ions are presented in Table 1, which includes only the electronic excited states associated with the configuration  $1s^2 2s^2 2p^n$ , where  $n = 2, 3, 4, 5$ . It can be found that for all considered ions, there exist electronic states

with energies close to the isomeric energy of the  $^{205}\text{Pb}$  nucleus. These states facilitate mixing between the nuclear ground state and the isomeric state.

The calculation of the electronic levels listed in Table 1 was performed by using the GRASP2018 package, which is based on a fully relativistic multiconfiguration Dirac–Hartree–Fock method [24]. This package is specifically designed for medium-to-heavy atomic systems and includes subprograms to calculate the relativistic wave functions, energy levels, hyperfine structures, and other atomic properties. In our calculation, the precision of these levels was systematically improved by applying an active set method and layer-by-layer calculations.

**Table 1.** Partial low-lying energy levels of the  $^{205}\text{Pb}^{76+}$ ,  $^{205}\text{Pb}^{75+}$ ,  $^{205}\text{Pb}^{74+}$ , and  $^{205}\text{Pb}^{73+}$  ions. For each ion, only the states with the ground-state configuration are presented.

Ions	Configuration	Angular Momentum $J$	Energy (eV)
$^{205}\text{Pb}^{76+}$	$2p^2$	0	0
	$2p^2$	1	2288
	$2p^2$	2	2306
	$2p^2$	2	4627
	$2p^2$	0	4701
$^{205}\text{Pb}^{75+}$	$2p^3$	3/2	0
	$2p^3$	3/2	2256
	$2p^3$	5/2	2279
	$2p^3$	1/2	2342
	$2p^3$	3/2	4605
$^{205}\text{Pb}^{74+}$	$2p^4$	2	0
	$2p^4$	0	71.34
	$2p^4$	1	2265
	$2p^4$	2	2283
	$2p^4$	0	4582
$^{205}\text{Pb}^{73+}$	$2p^5$	3/2	0
	$2p^5$	1/2	2247

For  $^{205}\text{Pb}^{76+}$ , the angular momentum of the electronic ground state  $J_g$  was zero. As a result, the nuclear ground and isomeric states did not split into sublevels. The total angular momenta were equal to the nuclear spins; specifically,  $F_g = 5/2$  and  $F_e = 1/2$ . For  $^{205}\text{Pb}^{75+}$ ,  $J_g = 3/2$ , the nuclear ground and isomeric states split into four levels with  $F_g = 1, 2, 3, 4$  and two levels with  $F_e = 1, 2$ , respectively. Similarly, for  $^{205}\text{Pb}^{74+}$ ,  $J_g = 2$ , the nuclear ground and isomeric states split into five levels with  $F_g = 1/2, 3/2, 5/2, 7/2, 9/2$  and two levels with  $F_e = 3/2, 5/2$ , respectively. Finally, for  $^{205}\text{Pb}^{73+}$ , with  $J_g = 3/2$ , the nuclear ground and isomeric states split into four levels with  $F_g = 1, 2, 3, 4$  and two levels with  $F_e = 1, 2$ , respectively.

The energy shifts due to NHM in  $^{205}\text{Pb}^{75+}$ ,  $^{205}\text{Pb}^{74+}$ , and  $^{205}\text{Pb}^{73+}$  were estimated to be to the order of 0.001–0.01 eV. Given that the nuclear transition energy was 2.329 keV, the impact of these shifts was negligible, and thus they are not discussed further. In our calculation, the magnetic and quadrupole moments of the nuclear ground state were taken to be  $0.71 \mu_N$  and 0.226 eb, respectively [22]. For the isomeric state, there were no available data for the magnetic and quadrupole moments. Therefore, the isomeric magnetic moment was estimated using the Schmidt model [28], yielding a value of  $0.64 \mu_N$ . For the isomeric quadrupole moment, a value of 1 eb was used to provide a magnitude estimate.

### 3.2. Mixing Coefficients in $^{205}\text{Pb}^{76+}$ , $^{205}\text{Pb}^{75+}$ , $^{205}\text{Pb}^{74+}$ , and $^{205}\text{Pb}^{73+}$ Ions

By means of the dressed hyperfine states, the nuclear ground states of the  $^{205}\text{Pb}^{76+}$ ,  $^{205}\text{Pb}^{75+}$ ,  $^{205}\text{Pb}^{74+}$ , and  $^{205}\text{Pb}^{73+}$  ions are represented by  $[[I_g(2p^n)J_g]F_gM_{F_g}]$ , where  $J_g$  denotes the angular momentum of electronic ground states in these ions. According to the expression of the mixing coefficients [Equation (7)], only those mixing coefficients corresponding to the hyperfine coupled bases with energies close to that of the hyperfine coupled basis  $|I_g(2p^n)J_g; F_gM_{F_g}\rangle$  are significant. Due to the large energy gaps between the hyperfine coupled bases  $|I_g(2p^n)J_g; F_gM_{F_g}\rangle$  and  $|I_e(2p^n)J_g; F_gM_{F_g}\rangle$  as well as  $|I_e(2p^n)J_e; F_gM_{F_g}\rangle$ , the mixing coefficients for the nuclear ground state  $[[I_g(2p^n)J_g]F_gM_{F_g}]$  are negligibly small and can be effectively approximated to be

$$[[I_g(2p^n)J_g]F_gM_{F_g}] = |I_g(2p^n)J_g; F_gM_{F_g}\rangle \quad (13)$$

for  $n = 2, 3, 4, 5$ . Here,  $J_e$  is the angular momentum of the electronic excited state.

Similarly, the isomeric states of the  $^{205}\text{Pb}^{76+}$ ,  $^{205}\text{Pb}^{75+}$ ,  $^{205}\text{Pb}^{74+}$ , and  $^{205}\text{Pb}^{73+}$  ions are described by the dressed hyperfine states  $[[I_e(2p^n)J_e]F_eM_{F_e}]$ . In  $^{205}\text{Pb}^{76+}$ , as shown in Table 1, the energy of the hyperfine coupled basis  $|I_e(2p^2)J_e; F_eM_{F_e}\rangle$  was close to those of the hyperfine coupled bases  $|I_g(2p^2)J_e = 1; F_eM_{F_e}\rangle$  and  $|I_g(2p^2)J_e = 2; F_eM_{F_e}\rangle$  (with 2306 eV of energy). However, since the nuclear transition type was E2, and  $J_g = 0$  for the  $^{205}\text{Pb}^{76+}$  ion, the mixing coefficient between  $|I_e(2p^2)J_e; F_eM_{F_e}\rangle$  and  $|I_g(2p^2)J_e = 1; F_eM_{F_e}\rangle$  was zero according to the angular momentum selection rules. As a result, the isomeric state of  $^{205}\text{Pb}^{76+}$   $[[I_e(2p^2)J_e]F_eM_{F_e}]$  contains only one dominant mixing coefficient, and it can be explicitly expressed as follows:

$$[[I_e(2p^2)J_e]F_eM_{F_e}] = |I_e(2p^2)J_e; F_eM_{F_e}\rangle + b_{76} |I_g(2p^2)J_e = 2; F_eM_{F_e}\rangle, \quad (14)$$

where  $b_{76}$  is the mixing coefficient between  $|I_e(2p^2)J_e; F_eM_{F_e}\rangle$  and  $|I_g(2p^2)J_e = 2; F_eM_{F_e}\rangle$ .

In  $^{205}\text{Pb}^{75+}$ , the hyperfine coupled basis  $|I_e(2p^3)J_e; F_eM_{F_e}\rangle$  had an energy comparable to those of the hyperfine coupled bases  $|I_g(2p^3)J_e = 3/2; F_eM_{F_e}\rangle$  (with 2256 eV of energy),  $|I_g(2p^3)J_e = 5/2; F_eM_{F_e}\rangle$ , and  $|I_g(2p^3)J_e = 1/2; F_eM_{F_e}\rangle$ . Thus, the isomeric state of  $^{205}\text{Pb}^{75+}$   $[[I_e(2p^3)J_e]F_eM_{F_e}]$  is composed of three dominant mixing coefficients:

$$[[I_e(2p^3)J_e]F_eM_{F_e}] = |I_e(2p^3)J_e; F_eM_{F_e}\rangle + b_{75,1} |I_g(2p^3)J_e = 3/2; F_eM_{F_e}\rangle + b_{75,2} |I_g(2p^3)J_e = 5/2; F_eM_{F_e}\rangle + b_{75,3} |I_g(2p^3)J_e = 1/2; F_eM_{F_e}\rangle, \quad (15)$$

where  $b_{75,1}$ ,  $b_{75,2}$ , and  $b_{75,3}$  are the mixing coefficients associated with the hyperfine coupled bases  $|I_g(2p^3)J_e = 3/2; F_eM_{F_e}\rangle$ ,  $|I_g(2p^3)J_e = 5/2; F_eM_{F_e}\rangle$ , and  $|I_g(2p^3)J_e = 1/2; F_eM_{F_e}\rangle$ , respectively.

For  $^{205}\text{Pb}^{74+}$ , since the energy of the hyperfine coupled basis  $|I_e(2p^4)J_e; F_eM_{F_e}\rangle$  was close to those of bases  $|I_g(2p^4)J_e = 1; F_eM_{F_e}\rangle$  and  $|I_g(2p^4)J_e = 2; F_eM_{F_e}\rangle$ , the isomeric state of  $^{205}\text{Pb}^{74+}$   $[[I_e(2p^4)J_e]F_eM_{F_e}]$  is therefore written as

$$[[I_e(2p^4)J_e]F_eM_{F_e}] = |I_e(2p^4)J_e; F_eM_{F_e}\rangle + b_{74,1} |I_g(2p^4)J_e = 1; F_eM_{F_e}\rangle + b_{74,2} |I_g(2p^4)J_e = 2; F_eM_{F_e}\rangle, \quad (16)$$

where  $b_{74,1}$  and  $b_{74,2}$  are the mixing coefficients corresponding to the hyperfine coupled bases  $|I_g(2p^4)J_e = 1; F_eM_{F_e}\rangle$  and  $|I_g(2p^4)J_e = 2; F_eM_{F_e}\rangle$ , respectively.

For  $^{205}\text{Pb}^{73+}$ , there is only one hyperfine coupled basis  $|I_g(2p^5)J_e = 1/2; F_e M_{F_e}\rangle$  whose energy is close to that of the hyperfine coupled basis  $|I_g(2p^5)J_g; F_e M_{F_e}\rangle$ . Consequently, the isomeric state of  $^{205}\text{Pb}^{73+}$   $|[I_e(2p^5)J_g]F_e M_{F_e}\rangle$  is given by

$$|[I_e(2p^5)J_g]F_e M_{F_e}\rangle = |I_e(2p^5)J_g; F_e M_{F_e}\rangle + b_{73}|I_g(2p^5)J_e = 1/2; F_e M_{F_e}\rangle, \quad (17)$$

where  $b_{73}$  is the mixing coefficient between  $|I_g(2p^5)J_e = 1/2; F_e M_{F_e}\rangle$  and  $|I_e(2p^5)J_g; F_e M_{F_e}\rangle$ .

Using Equation (7), the mixing coefficients were numerically calculated, and they are presented in Table 2. One can see that the mixing coefficients  $b_{76}$  and  $b_{75,3}$  were on the order of  $10^{-5}$ , whereas the others were relatively smaller and on the order of  $10^{-6}$ . This is mainly because the energy gaps associated with the mixing coefficients  $b_{76}$  and  $b_{75,3}$  were smaller compared with those of the other mixing coefficients.

**Table 2.** Mixing coefficients of the isomeric states  $|[I_e(2p^2)J_g]F_e M_{F_e}\rangle$ ,  $|[I_e(2p^3)J_g]F_e M_{F_e}\rangle$ ,  $|[I_e(2p^4)J_g]F_e M_{F_e}\rangle$ , and  $|[I_e(2p^5)J_g]F_e M_{F_e}\rangle$  for different values of  $F_e$ .

Isomeric State	Total Angular Momentum $F_e$	Mixing Coefficients ( $\times 10^{-5}$ )
$ [I_e(2p^2)J_g]F_e M_{F_e}\rangle$	1/2	$b_{76} = -2.74$
$ [I_e(2p^3)J_g]F_e M_{F_e}\rangle$	1	$b_{75,1} = -0.16, b_{75,2} = 0.85,$ $b_{75,3} = 0$
	2	$b_{75,1} = -0.32, b_{75,2} = 0.93,$ $b_{75,3} = -2.16$
$ [I_e(2p^4)J_g]F_e M_{F_e}\rangle$	3/2	$b_{74,1} = -0.15, b_{74,2} = 0.56$
	5/2	$b_{74,1} = -0.47, b_{74,2} = 0.92$
$ [I_e(2p^5)J_g]F_e M_{F_e}\rangle$	1	$b_{73} = 0$
	2	$b_{73} = 0.47$

### 3.3. Nuclear Transitions in $^{205}\text{Pb}^{76+}$ , $^{205}\text{Pb}^{75+}$ , $^{205}\text{Pb}^{74+}$ , and $^{205}\text{Pb}^{73+}$ Ions

The numerically determined mixing coefficients allowed for the calculation of nuclear transition rates  $\Gamma$  via the NHM effect by employing Equation (10). The half-life of the isomeric state is related to the transition rate by the relation  $T_{1/2} = \ln 2/\Gamma$ . The corresponding results are presented in Table 3. For each ion, the nuclear ground states  $|[I_g(2p^n)J_g]F_g M_{F_g}\rangle$  and isomeric states  $|[I_e(2p^n)J_g]F_e M_{F_e}\rangle$  are uniquely characterized by their total angular momenta  $F_g$  and  $F_e$ . Accordingly, the nuclear transition channels from the isomeric states  $|[I_e(2p^n)J_g]F_e M_{F_e}\rangle$  with  $F_e = i$  to the ground states  $|[I_g(2p^n)J_g]F_g M_{F_g}\rangle$  with  $F_g = j$  are denoted by  $F_e = i \rightarrow F_g = j$  in this table and in the following discussions.

Due to the angular momentum selection rules, the M1 transition for the nuclear decay in  $^{205}\text{Pb}^{76+}$  remains forbidden, and nuclear decay occurs solely through the E2 transition. In the other ions, the NHM effect allows the opening of M1 transitions. Nevertheless, the NHM effect significantly altered the isomeric decay process in  $^{205}\text{Pb}^{76+}$ , reducing the lifetime of the isomeric state by over two orders of magnitude from 15 min to 1.6 s.

For  $^{205}\text{Pb}^{75+}$ , there were seven possible decay channels, with the corresponding decay rates being from the order of  $10^{-2}$  to 10 per second. The nuclear decay occurred through either M1 or E2 transitions. Among these decay channels, the M1 transitions were more efficient than the E2 transitions. The most efficient decay channel was  $F_e = 2 \rightarrow F_g = 2$ , in which the lifetime of the isomeric state was reduced by more than four orders of magnitude from 15 min to 39 ms.

**Table 3.** Nuclear transitions via the NHM effect for different channels in the  $^{205}\text{Pb}^{76+}$ ,  $^{205}\text{Pb}^{75+}$ ,  $^{205}\text{Pb}^{74+}$ , and  $^{205}\text{Pb}^{73+}$  ions. The forbidden  $M1$  transitions in the bare nucleus were open in the latter three ions.

Ions	Transition	Type	Rate ( $\text{s}^{-1}$ )	$T_{1/2}$
$^{205}\text{Pb}^{76+}$	$F_e = 1/2 \rightarrow F_g = 5/2$	$E2$	$4.3 \times 10^{-1}$	1.6 s
$^{205}\text{Pb}^{75+}$	$F_e = 1 \rightarrow F_g = 1$	$M1$	$4.5 \times 10^{-1}$	1.5 s
	$F_e = 1 \rightarrow F_g = 2$	$M1$	1.2	0.60 s
	$F_e = 1 \rightarrow F_g = 3$	$E2$	$1.7 \times 10^{-2}$	40 s
	$F_e = 2 \rightarrow F_g = 1$	$M1$	7.8	89 ms
	$F_e = 2 \rightarrow F_g = 2$	$M1$	18	39 ms
	$F_e = 2 \rightarrow F_g = 3$	$M1$	2.4	0.29 s
	$F_e = 2 \rightarrow F_g = 4$	$E2$	$1.7 \times 10^{-1}$	4.1 s
$^{205}\text{Pb}^{74+}$	$F_e = 3/2 \rightarrow F_g = 1/2$	$M1$	$3.1 \times 10^{-1}$	2.2 s
	$F_e = 3/2 \rightarrow F_g = 3/2$	$M1$	$2.8 \times 10^{-2}$	25 s
		$E2$	$2.1 \times 10^{-2}$	33 s
		$M1$	1.6	0.43 s
	$F_e = 3/2 \rightarrow F_g = 5/2$	$M1$	$6.6 \times 10^{-3}$	1.8 min
	$F_e = 3/2 \rightarrow F_g = 7/2$	$E2$	$4.7 \times 10^{-2}$	15 s
	$F_e = 5/2 \rightarrow F_g = 1/2$	$E2$	$7.3 \times 10^{-1}$	0.94 s
	$F_e = 5/2 \rightarrow F_g = 3/2$	$M1$	$4.2 \times 10^{-3}$	2.8 min
	$F_e = 5/2 \rightarrow F_g = 5/2$	$E2$	6.0	0.12 s
$F_e = 5/2 \rightarrow F_g = 7/2$	$M1$	$1.7 \times 10^{-4}$	69 min	
$^{205}\text{Pb}^{73+}$	$F_e = 2 \rightarrow F_g = 1$	$M1$	$7.4 \times 10^{-1}$	0.93 s
	$F_e = 2 \rightarrow F_g = 2$	$M1$	$9.7 \times 10^{-1}$	0.72 s
	$F_e = 2 \rightarrow F_g = 3$	$M1$	$7.7 \times 10^{-1}$	0.90 s
	$F_e = 2 \rightarrow F_g = 4$	$E2$	$2.9 \times 10^{-2}$	24 s

For  $^{205}\text{Pb}^{74+}$ , there were nine possible decay channels, with the corresponding decay rates being from the order of  $10^{-4}$  to 1 per second. In the  $F_e = 3/2 \rightarrow F_g = 3/2$  decay channel, there was no dominant transition type. Instead, the rates for the  $M1$  and  $E2$  transitions were comparable. Therefore, the transition rates for both  $M1$  and  $E2$  are listed in Table 3. In the  $F_e = 5/2 \rightarrow F_g = 5/2$  decay channel, the  $M1$  transition was allowed by the angular momentum selection rules, but this channel was dominated by the  $E2$  transition. The most efficient decay channel was  $F_e = 5/2 \rightarrow F_g = 7/2$ , where the isomeric lifetime was reduced by more than three orders of magnitude from 15 min to 0.12 s.

For  $^{205}\text{Pb}^{73+}$ , since the mixing coefficient  $b_{73}$  for  $F_e = 1$  was zero (see Table 2), the nuclear transitions  $F_e = 1 \rightarrow F_g = j$  were nearly identical to that of the bare nucleus. Therefore, these transitions are not included in Table 3, and four possible decay channels are presented in this table. The isomeric decay via the  $F_e = 2 \rightarrow F_g = 2$  channel was most efficient, and the isomeric lifetime was reduced by about three orders of magnitude from 15 min to 0.72 s.

### 3.4. Potential Experimental Verification

In this section, we propose a potential experimental scheme to verify the NHM effect using  $^{205}\text{Pb}$  ions. These ions could be created and stored in electron beam ion traps and subsequently excited by X-ray free electron lasers (XFELs) [29]. Since the  $M1$  transition channel is typically much more efficient than the  $E2$  channel, we focus on the optical excitation of the  $^{205}\text{Pb}$  isomers via the  $M1$  channel. The excitation probability involving the NHM effect can be calculated by following a method similar to Equation (17) in [30]:



$$P_{\text{exc}} = \frac{4\pi}{9} B_{\text{eff}}(M1, g \rightarrow e) E_0^2 \left| \int_0^T f(t) \sin(\omega_0 t) e^{i\omega t} dt \right|^2, \quad (18)$$

where  $E_0$ ,  $\omega_0$ , and  $f(t)$  are the amplitude, angular frequency, and envelope function of the laser pulse, respectively.  $B_{\text{eff}}(M1, g \rightarrow e)$  is a generalized nuclear reduced transition probability, defined by

$$B_{\text{eff}}(M1, g \rightarrow e) = \frac{3(2F_e + 1)}{4\pi} |\langle [I_g \gamma_g J_g] F_g || \mathcal{O}^{(M1)} + \mathcal{M}^{(M1)} || [I_e \gamma_g J_g] F_e \rangle|^2, \quad (19)$$

and it can be determined by the nuclear  $M1$  transition rate  $\Gamma$  [Equation (10)] as follows:

$$B_{\text{eff}}(M1, g \rightarrow e) = \frac{2F_e + 1}{2F_g + 1} \frac{9\Gamma}{16\pi} \left( \frac{c}{\omega} \right)^3. \quad (20)$$

As an example, consider the excitation of the  $^{205}\text{Pb}^{75+}$  ion from  $F_g = 2$  to  $F_e = 2$  by 2.329 keV X-ray pulses. We utilized the parameters of the European XFEL [31], which produces X-ray pulses in bunches. Each bunch lasts 0.6 ms and contains 2700 individual pulses, each with a duration of 100 fs. The bunches are separated by a 100 ms gap, and thus there are 10 bunches every second. Each pulse carries approximately  $10^{13}$  X-ray photons and can reach an intensity of over  $10^{18}$  W/cm<sup>2</sup>. Using Equation (18), we calculated the nuclear excitation probability to be approximately  $1.7 \times 10^{-4}$  per ion per bunch. Assuming that there are 600  $^{205}\text{Pb}^{75+}$  ions, we would expect approximately one nuclear excitation per second (i.e., every 10 bunches). The lifetime of the isomeric state was 39 ms, and thus if excitation occurs during a pulse bunch, a decay photon should be emitted within the following gap. The decay time can be measured relative to the time zero defined by the previous bunch.

In the absence of the NHM effect, virtually no isomeric excitation would be expected, and thus the detection of a decay photon would provide direct evidence for the presence of the NHM effect. With the continued development of next-generation XFEL facilities, such as the Shanghai High Repetition Rate XFEL and the Extreme Light Facility (SHINE) [32], data collection efficiency can be significantly enhanced due to even higher repetition rates.

#### 4. Conclusions

The theory of the NHM effect was reformulated using dressed hyperfine states. The partial energy level structures of the  $^{205}\text{Pb}^{76+}$ ,  $^{205}\text{Pb}^{75+}$ ,  $^{205}\text{Pb}^{74+}$ , and  $^{205}\text{Pb}^{73+}$  ions as well as the nuclear transitions induced by the NHM effect in these ions were investigated. Significant NHM effects were predicted in these ions, as they each have electronic energy levels close to the energy of the nuclear isomeric state. Specifically, in  $^{205}\text{Pb}^{76+}$ , the lifetime of the isomeric state was reduced by more than two orders of magnitude due to the NHM effect, while in  $^{205}\text{Pb}^{75+}$ , the lifetime was reduced by over four orders of magnitude. For  $^{205}\text{Pb}^{74+}$  and  $^{205}\text{Pb}^{73+}$ , the lifetime was reduced by over three orders of magnitude. It is important to note that  $^{205}\text{Pb}^{76+}$  and  $^{205}\text{Pb}^{74+}$  do not have unpaired valence electrons. This suggests that it is the active valence electrons, rather than unpaired electrons, which play a critical role in the NHM effect. Our findings enhance the understanding of the NHM effect and are expected to aid in the experimental validation of the NHM effect in the  $^{205}\text{Pb}$  nucleus.

**Author Contributions:** Conceptualization, software, formal analysis, writing—original draft preparation, and writing—review and editing, W.W.; conceptualization and writing—review and editing, Y.L.; conceptualization, validation, formal analysis, and writing—review and editing, X.W. All authors have read and agreed to the published version of the manuscript.

**Funding:** X.W. was funded by the National Natural Science Foundation of China (Grant Nos. 12474484, U2330401, and 12088101); Y.L. was funded by the Innovation Program for Quantum Science and Technology (Grant No. 2023ZD0300700) and the National Natural Science Foundation of China (Grant No. 12274107); and W.W. was funded by the Postdoctoral Fellowship Program of CPSF (Grant No. GZC20240359).

**Data Availability Statement:** Data are contained within this article.

**Conflicts of Interest:** The authors declare no conflicts of interest.

## References

- Kozlov, M.G.; Safronova, M.S.; Crespo López-Urrutia, J.R.; Schmidt, P.O. Highly Charged Ions: Optical Clocks and Applications in Fundamental Physics. *Rev. Mod. Phys.* **2018**, *90*, 045005. [[CrossRef](#)]
- Eides, M.I.; Grotch, H.; Shelyuto, V.A. Theory of Light Hydrogenlike Atoms. *Phys. Rep.* **2001**, *342*, 63–261. [[CrossRef](#)]
- Shabaev, V.M.; Glazov, D.A.; Plunien, G.; Volotka, A.V. Theory of Bound-Electron g Factor in Highly Charged Ions. *J. Phys. Chem. Ref. Data* **2015**, *44*, 031205. [[CrossRef](#)]
- Sturm, S.; Vogel, M.; Köhler-Langes, F.; Quint, W.; Blaum, K.; Werth, G. High-Precision Measurements of the Bound Electron's Magnetic Moment. *Atoms* **2017**, *5*, 4. [[CrossRef](#)]
- Beiersdorfer, P. Laboratory X-ray Astrophysics. *Annu. Rev. Astron. Astrophys.* **2003**, *41*, 343–390. [[CrossRef](#)]
- Lyuboshitz, V.L.; Onishchuk, V.A.; Podgoretskij, M.I. Some Interference Effects Due to the Mixing of Quantum Levels by External Fields. *Sov. J. Nucl. Phys.* **1966**, *3*, 420.
- Szerypo, J.; Barden, R.; Kalinowski, Ł.; Kirchner, R.; Klepper, O.; Plochocki, A.; Roeckl, E.; Rykaczewski, K.; Schardt, D.; Żylicz, J. Low-Lying Levels in  $^{104}\text{In}$  and a Problem of Spin-mixing in Hyperfine Fields. *Nucl. Phys. A* **1990**, *507*, 357–370. [[CrossRef](#)]
- Wycech, S.; Żylicz, J. Predictions for Nuclear Spin Mixing in Magnetic Fields. *Acta Phys. Pol. B* **1993**, *24*, 637–647.
- Wu, C.S.; Willets, L. Muonic Atoms and Nuclear Structure. *Annu. Rev. Nucl. Part. Sci.* **1969**, *19*, 527–606. [[CrossRef](#)]
- Hitlin, D.; Bernow, S.; Devons, S.; Duerdoth, I.; Kast, J.W.; Macagno, E.R.; Rainwater, J.; Wu, C.S.; Barrett, R.C. Muonic Atoms. I. Dynamic Hyperfine Structure in the Spectra of Deformed Nuclei. *Phys. Rev. C* **1970**, *1*, 1184. [[CrossRef](#)]
- Michel, N.; Oreshkina, N.S. Higher-order Corrections to the Dynamic Hyperfine Structure of Muonic Atoms. *Phys. Rev. A* **2019**, *99*, 042501. [[CrossRef](#)]
- Karpeshin, F.F.; Wycech, S.; Band, I.M.; Trzhaskovskaya, M.B.; Pfützner, M.; Żylicz, J. Rates of Transitions between the Hyperfine-splitting Components of the Ground-state and the 3.5 eV Isomer in  $^{229}\text{Th}^{89+}$ . *Phys. Rev. C* **1998**, *57*, 3085. [[CrossRef](#)]
- Pachucki, K.; Wycech, S.; Żylicz, J.; Pfützner, M. Nuclear-spin Mixing Oscillations in  $^{229}\text{Th}^{89+}$ . *Phys. Rev. C* **2001**, *64*, 064301. [[CrossRef](#)]
- Tkalya, E.V.; Nikolaev, A.V. Magnetic Hyperfine Structure of the Ground-state Doublet in Highly Charged Ions  $^{229}\text{Th}^{89+,87+}$  and the Bohr-Weisskopf Effect. *Phys. Rev. C* **2016**, *94*, 014323. [[CrossRef](#)]
- Shabaev, V.M.; Glazov, D.A.; Ryzhkov, A.M.; Brandau, C.; Plunien, G.; Quint, W.; Volchkova, A.M.; Zinenko, D.V. Ground-State g Factor of Highly Charged  $^{229}\text{Th}$  Ions: An Access to the M1 Transition Probability between the Isomeric and Ground Nuclear States. *Phys. Rev. Lett.* **2022**, *128*, 043001. [[CrossRef](#)]
- Jin, J.; Bekker, H.; Kirschbaum, T.; Litvinov, Y.A.; Pálffy, A.; Sommerfeldt, J.; Surzhykov, A.; Thierolf, P.G.; Budker, D. Excitation and Probing of Low-energy Nuclear States at High-energy Storage Rings. *Phys. Rev. Res.* **2023**, *5*, 023134. [[CrossRef](#)]
- Wang, W.; Wang, X. Substantial Nuclear Hyperfine Mixing Effect in Boronlike  $^{205}\text{Pb}$  Ions. *Phys. Rev. Lett.* **2024**, *133*, 032501. [[CrossRef](#)] [[PubMed](#)]
- Zhang, H.; Li, T.; Wang, X. Highly Nonlinear Light-Nucleus Interaction. *Phys. Rev. Lett.* **2024**, *133*, 152503. [[CrossRef](#)]
- Tiedau, J.; Okhapkin, M.V.; Zhang, K.; Thielking, J.; Zitzer, G.; Peik, E.; Schaden, F.; Pronebner, T.; Morawetz, I.; Toscani De Col, L.; et al. Laser Excitation of the Th-229 Nucleus. *Phys. Rev. Lett.* **2024**, *132*, 182501. [[CrossRef](#)]
- Elwell, R.; Schneider, C.; Jeet, J.; Terhune, J.E.S.; Morgan, H.W.T.; Alexandrova, A.N.; Tran Tan, H.B.; Derevianko, A.; Hudson, E.R. Laser Excitation of the  $^{229}\text{Th}$  Nuclear Isomeric Transition in a Solid-State Host. *Phys. Rev. Lett.* **2024**, *133*, 013201. [[CrossRef](#)]
- Zhang, C.; Ooi, T.; Higgins, J.S.; Doyle, J.F.; von der Wense, L.; Beeks, K.; Leitner, A.; Kazakov, G.A.; Li, P.; Thierolf, P.G.; et al. Frequency Ratio of the  $^{229\text{m}}\text{Th}$  Nuclear Isomeric Transition and the  $^{87}\text{Sr}$  Atomic Clock. *Nature* **2024**, *633*, 63–70. [[CrossRef](#)] [[PubMed](#)]
- Nuclear Structure and Decay Databases. Available online: <https://www.nndc.bnl.gov/> (accessed on 20 October 2024).
- Wang, W.; Zou, F.; Fritzsche, S.; Li, Y. Isomeric Population Transfer of the  $^{229}\text{Th}$  Nucleus via Hyperfine Electronic Bridge. *Phys. Rev. Lett.* **2024**, *133*, 223001. [[CrossRef](#)] [[PubMed](#)]
- Fischer, C.F.; Gaigalas, G.; Jönsson, P.; Bieroń, J. GRASP2018—A Fortran 95 version of the General Relativistic Atomic Structure Package. *Comput. Phys. Commun.* **2019**, *237*, 184–187. [[CrossRef](#)]
- Schwartz, C. Theory of Hyperfine Structure. *Phys. Rev.* **1955**, *97*, 380. [[CrossRef](#)]

26. Fritzsche, S. The Ratip Program for Relativistic Calculations of Atomic Transition, Ionization and Recombination Properties. *Comput. Phys. Commun.* **2012**, *183*, 1525–1559. [[CrossRef](#)]
27. Alder, K.; Bohr, A.; Huus, T.; Mottelson, B.; Winther, A. Study of Nuclear Structure by Electromagnetic Excitation with Accelerated Ions. *Rev. Mod. Phys.* **1956**, *28*, 432. [[CrossRef](#)]
28. Schmidt, T. Über die magnetischen Momente der Atomkerne. *Z. Phys. A* **1937**, *106*, 358–361. [[CrossRef](#)]
29. Bernitt, S.; Brown, G.V.; Rudolph, J.K.; Steinbrügge, R.; Graf, A.; Leutenegger, M.; Epp, S.W.; Eberle, S.; Kubiček, K.; Mäckel, V.; et al. An Unexpectedly Low Oscillator Strength as the Origin of the Fe XVII Emission Problem. *Nature* **2012**, *492*, 225–228. [[CrossRef](#)]
30. Wang, W.; Wang, X. Quantum Theory of Isomeric Excitation of  $^{229}\text{Th}$  in Strong Laser Fields. *Phys. Rev. Res.* **2023**, *5*, 043232. [[CrossRef](#)]
31. Izquierdo, M. *Scientific Instrument Soft X-Ray Port (SXP). Part A: Science Cases*; XFEL.EU TR-2022-001A; European X-Ray Free-Electron Laser Facility GmbH: Schenefeld, Germany, 2022.
32. Liu, T.; Huang, N.; Yang, H.; Qi, Z.; Zhang, K.; Gao, Z.; Chen, S.; Feng, C.; Zhang, W.; Luo, H.; et al. Status and Future of the Soft X-ray Free-Electron Laser Beamline at the SHINE. *Front. Phys.* **2023**, *11*, 1172368. [[CrossRef](#)]

**Disclaimer/Publisher's Note:** The statements, opinions and data contained in all publications are solely those of the individual author(s) and contributor(s) and not of MDPI and/or the editor(s). MDPI and/or the editor(s) disclaim responsibility for any injury to people or property resulting from any ideas, methods, instructions or products referred to in the content.